Journal of Structural Geology, Vol 13, No 7, pp 859 to 864, 1991
Printed in Great Britain

0191-8141/91 $03 00+0 00

The analysis of progressive deformation from an inscribed grid

NEIL S. MANCKTELOW

Geologisches Institut, ETH-Zentrum, CH-8092 Zurich, Switzerland

(*Received* 15 *June* 1990; *accepted in revised form* 8 *February* 1991)

Abstract—The analysis of deformed inscribed grids (or equivalent particle points) from scale-model experiments permits a very detailed investigation of the progressive development of geological structures. Numerical methods to calculate values related to the finite deformation (strain ellipse, finite rotation and displacement) and to the instantaneous deformation rate (velocity, stretching rate, vorticity, kinematical vorticity number, spin) from the co-ordinates of digitized grid nodes are summarized. These values can be plotted directly (e.g. as principal strain axes) or their magnitudes can be contoured across the surface of the model. Particular consideration is given to the practical advantages of separating the overall heterogeneous deformation into an average homogeneous component and an additional heterogeneous component representing deviations away from this standard state. This approach corresponds closely to the concept, commonly used in the analysis of mechanical instability, of a perturbation superimposed on a basic steady flow.

INTRODUCTION

ONE significant advantage of experimental studies of deformation structures lies in the ability to analyse the progressive displacement and deformation history in a detail which is unattainable in natural field examples. The potential of this approach could only be fully exploited with the advent of digitizing tablets and digital computers as, without these aids, the calculations are too tedious to be repeated hundreds of times across the surface of a single scale-model. Many earlier experiments utilized circles imprinted on the model surface (Ramberg 1959, Ghosh 1975, Ghosh & Ramberg 1976, Gairola 1978). This approach has the advantage of immediately visualizing the accumulated finite strain, but is not well suited to a more extensive analysis of the progressive deformation. In those cases where a grid was inscribed, the deformed grids were often used as excellent visual aids (Ramberg 1961, 1963, 1964, Hudleston 1973, Neurath & Smith 1982), but only rarely were they further utilized for quantitative analysis (Dixon 1974, Cobbold 1975). Fine grids have also been introduced between split rock cylinders to investigate strain heterogeneity on a grain scale during experimental rock deformation (Fitz Gerald & Chopra 1984) and pioneering studies of microfabric development using analogue materials have also used scattered opaque particles to determine the strain distribution (Means 1983).

This paper describes numerical routines for the extensive analysis of digitized grid nodes (Fig. 1) or particle points. These routines have been implemented as a freely available, menu-driven program for Apple Macintosh computers. The implementation is ideally suited to experiments where direct observation can be made during deformation, as, for example, in many analogue deformation machines (Cobbold 1975, Means 1983, Mancktelow 1988).

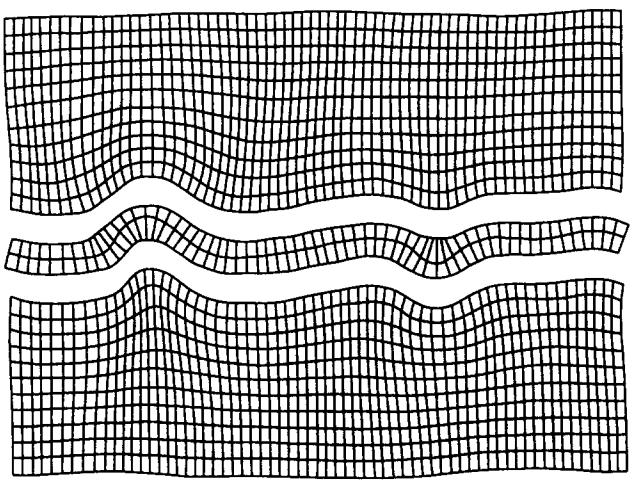

Fig. 1. Plot of the digitized deformed grid from a single-layer fold experiment at 25% bulk shortening. Layer and matrix were constructed of paraffin wax with different melting point ranges, to give an effective viscosity contrast of *ca* 30:1. Deformation geometry was pure shear. The grids for layer and matrix, which are shown exploded in the figure for clarity, were digitized separately as there has been slip along the layer–matrix interface. All further figures in this paper relate to this deformed grid, which records a particular instant in the progressive deformation history.

GENERAL BACKGROUND

The analysis of deformed grids is clearly based on the geometry of finite and infinitesimal strain, which is thoroughly described in many standard texts on continuum mechanics and the theory of plasticity (e.g. Jaeger 1962, Biot 1965, Malvern 1969, Chakrabarty 1987). Results are presented here in a form that is convenient for numerical solution using the available data, namely the co-ordinates of the grid nodes digitized at discrete intervals during a progressive deformation.

First consider the most general case. Let $\mathbf{q}_i$ denote the components of some vector quantity at the point P,

whose position at a particular time t is given by the co-ordinates $\mathbf{x}_i$, and whose position at time $t = 0$ was $\mathbf{x}_i^0$. Consider also a neighbouring point Q at an infinitesimal distance from P, the current co-ordinates of Q being $\mathbf{x}_i + \delta\mathbf{x}_i$. The change in value of the vector quantity $\mathbf{q}_i$ in going from P to Q is given by:

$$\delta\mathbf{q}_i = \frac{\partial\mathbf{q}_i}{\partial\mathbf{x}_j}\delta\mathbf{x}_j, \tag{1}$$

where $\partial\mathbf{q}_i/\partial\mathbf{x}_j$ represent the components of the gradient tensor in $\mathbf{q}$ at the point P. If these gradient components do not vary with position $\mathbf{x}_i$, then the distribution is homogeneous, the requirement that the distance between P and Q be infinitesimal can be relaxed, and (1) will be true for any two points. If the gradients in $\mathbf{q}_i$ vary slowly with $\mathbf{x}_i$, then these gradients may be considered approximately constant for a small region around P and the variation in the quantity $\mathbf{q}_i$ can be considered in terms of a series of approximately homogeneous domains.

For deformed grids, the analysis is restricted to two dimensions, and the quantities of interest are the displacement, the velocity and the acceleration. These quantities are related to position, as in (1) above, by the respective displacement, velocity and acceleration gradients in the two co-ordinate directions x_1 and x_2. The gradients can be calculated directly at any point P by fitting a smooth surface to the variation in q_1 with position (x_1, x_2), determining the gradients by differentiation in the x_1 direction $\partial q_1/\partial x_1$ and in the x_2 direction $\partial q_1/\partial x_2$, and then repeating the exercise for q_2 to give $\partial q_2/\partial x_1$ and $\partial q_2/\partial x_2$. In practice, this can be done very efficiently using a bi-cubic spline interpolation (e.g. Ahlberg *et al.* 1967), if the known values of $\mathbf{q}_i$ correspond to positions on a rectangular grid. The gradient values required generally relate to the deformed state and the deformed grid is unlikely to be rectangular. The initial undeformed grid may easily be made rectangular, however, and if the gradients are first calculated relative to the initial position co-ordinates $\mathbf{x}_i^0$, a simple relation can be established between these gradient components and the components relative to the current co-ordinates $\mathbf{x}_i$. The co-ordinates $\mathbf{x}_i$ are related to their initial position by the co-ordinate transformation

$$\mathbf{x}_i = \mathbf{c}_{ij}\mathbf{x}_j^0 + \mathbf{d}_i.$$

The difference in position between two neighbouring points is, therefore,

$$\delta\mathbf{x}_i = \mathbf{c}_{ij}\delta\mathbf{x}_j^0$$

or, on rearrangement,

$$\delta\mathbf{x}_i^0 = \mathbf{b}_{ij}\delta\mathbf{x}_j, \tag{2}$$

where the matrix represented by the components $\mathbf{b}_{ij}$ is simply the inverse of the matrix with components $\mathbf{c}_{ij}$. The relationship, analogous to (1) above, between the value of $\mathbf{q}_i$ and the initial co-ordinates $\mathbf{x}_i^0$ is:

$$\delta\mathbf{q}_i = \frac{\partial\mathbf{q}_i}{\partial\mathbf{x}_j^0}\delta\mathbf{x}_j^0. \tag{3}$$

Substituting for $\delta\mathbf{x}_j^0$ using (2) gives:

$$\delta\mathbf{q}_i = \frac{\partial\mathbf{q}_i}{\partial\mathbf{x}_j^0}\mathbf{b}_{jk}\delta\mathbf{x}_k \tag{4}$$

and comparing equation (4) to equation (1), it is clear that the gradient matrix components relative to current co-ordinates is the same as that obtained by post-multiplying the gradient matrix relative to original co-ordinates by the Eulerian co-ordinate transformation matrix $\mathbf{b}_{jk}$, which relates the current co-ordinates to their initial position (cf. equation 60 in Hsu 1967).

If the initial grid is perfectly rectangular, the gradients at any point can be calculated in one pass, fitting the bi-cubic spline surface to the variation in $\mathbf{q}_i$ across the whole surface. As the interpolated surface is composed of a series of cubic polynomial segments in the x_1 and x_2 co-ordinate directions, the first and second derivatives in these directions are continuously and easily calculated. In practice, inscribed grids are often only approximately rectangular. To allow for this experimental inaccuracy, calculation can be restricted to a moving window of elements, where gradients are only determined within the central element (with necessary exceptions for edge and corner elements of the whole grid) and values at shared edge and node points are averaged over adjacent elements.

The main advantage of this direct method using a bi-cubic spline surface is that values can be obtained at any point across the grid surface, allowing for interpolation between grid nodes. The smoothing effect of surface fitting is generally an advantage, but can be a disadvantage when real discontinuities occur in the model, for example along material interfaces. The method can obviously not be applied when the initial grid is far from rectangular: more general (and more calculation intensive) methods of surface-fitting must be employed.

Alternatively, use can be made of the concept of approximate local homogeneity over a small area. If the gradient components $\partial\mathbf{q}_i/\partial\mathbf{x}_j$ can be assumed to remain constant in value over this small area, then relation (1) gives two equations in four unknowns. Clearly, the values of $\mathbf{q}_i$ at some other point Q′ are also required to give four equations in four unknowns, and a unique solution. The three points P, Q and Q′ together build a triangle, which is the smallest surface element (these points should not, of course, be colinear), and the gradient components in the x_1 and x_2 directions of this small surface element can be readily determined. Every quadrilateral element of a grid can be divided into four such triangles.

Consider first the equations for δq_1 (in each case, $\delta x_1'$, $\delta x_2'$ and $\delta q_1'$ indicate increments measured between points P and Q′, rather than between points P and Q):

$$\begin{pmatrix}\delta x_1 & \delta x_2\\ \delta x_1' & \delta x_2'\end{pmatrix}\begin{pmatrix}\partial q_1/\partial x_1\\ \partial q_1/\partial x_2\end{pmatrix} = \begin{pmatrix}\delta q_1\\ \delta q_1'\end{pmatrix}. \tag{5}$$

Solution is trivial, by matrix inversion, and is given by:

$$\begin{pmatrix}\partial q_1/\partial x_1\\ \partial q_1/\partial x_2\end{pmatrix} = \frac{1}{D}\begin{pmatrix}\delta x_2' & -\delta x_2\\ -\delta x_1' & \delta x_1\end{pmatrix}\begin{pmatrix}\delta q_1\\ \delta q_1'\end{pmatrix}, \tag{6}$$

where D is the determinant, that is,

$$D = \delta x_1 \delta x_2' - \delta x_1' \delta x_2$$

which will be non-zero if the points P, Q and Q′ are not colinear. The solution for the gradient components related to the δq_2 values is completely analogous:

$$\begin{pmatrix} \partial q_2/\partial x_1 \\ \partial q_2/\partial x_2 \end{pmatrix} = \frac{1}{D} \begin{pmatrix} \delta x_2' & -\delta x_2 \\ -\delta x_1' & \delta x_1 \end{pmatrix} \begin{pmatrix} \delta q_2 \\ \delta q_2' \end{pmatrix}. \quad (7)$$

This solution gives the gradients in terms of the *deformed* position co-ordinates $\partial \mathbf{q}_i/\partial \mathbf{x}_j$, but the result for gradients relative to the *initial* co-ordinates $\partial \mathbf{q}_i/\partial \mathbf{x}_j^0$ is identical in form, and can readily be obtained by simply substituting values of $\delta \mathbf{x}_i^0$ for the equivalent values of $\delta \mathbf{x}_i$ in (6) and (7).

The use of three points permits a unique solution for the gradients. If more points are included, the problem is overdetermined and a least-squares 'best-fit' solution to the set of linear equations is required (Lawson & Hanson 1974). This allows an 'average' value to be calculated for each quadrilateral grid element with four nodal points. An example is given in Fig. 2, where the average displacement gradients were calculated for each grid element and from these the average finite strain (see below). When applied to all nodes of the grid, this least-squares method can also be used to determine an average bulk 'homogeneous' value for the digitized grid surface as a whole.

FINITE STRAIN

Finite strain is related to variations in the displacement of particles, and thus directly to the displacement gradient tensor. As translation alone does not produce a change in shape, the analysis of finite strain around a point P can be simplified by tying the origin to this material point (so-called *material co-ordinates*), such that P always has co-ordinates (0, 0). In this case, the general relation (3) reduces to:

$$\mathbf{u}_i = \frac{\partial \mathbf{u}_i}{\partial \mathbf{x}_j^0} \mathbf{x}_j^0, \quad (8)$$

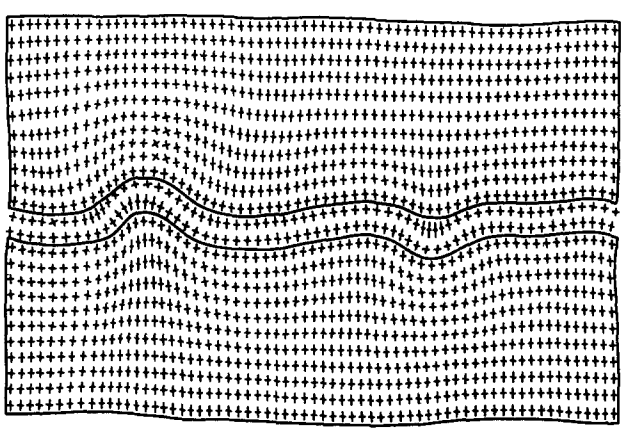

Fig. 2. Principal axes of the average finite strain ellipse for each quadrilateral grid element, calculated by the least-squares best-fit solution of the overdetermined set of linear equations (see text).

where $\mathbf{u}_i$ is the displacement vector of point Q relative to its initial position and $\mathbf{x}_j^0$ are the *initial* co-ordinates of point Q, established within the material co-ordinate system fixed to P. The position of point Q in the deformed state $\mathbf{x}_i$ is, of course, equal to the original co-ordinates $\mathbf{x}_i^0$ plus the displacements $\mathbf{u}_i$, hence:

$$\mathbf{x}_i = \mathbf{x}_i^0 + \mathbf{u}_i = \mathbf{x}_i^0 + \frac{\partial \mathbf{u}_i}{\partial \mathbf{x}_j^0} \mathbf{x}_j^0$$

which, in full matrix form, gives:

$$\begin{pmatrix} x_1 \\ x_2 \end{pmatrix} = \begin{pmatrix} 1 + \dfrac{\partial u_1}{\partial x_1^0} & \dfrac{\partial u_1}{\partial x_2^0} \\ \dfrac{\partial u_2}{\partial x_1^0} & 1 + \dfrac{\partial u_2}{\partial x_2^0} \end{pmatrix} \begin{pmatrix} x_1^0 \\ x_2^0 \end{pmatrix} \quad (9)$$

(e.g. Hsu 1967, equation 58). This is the co-ordinate transformation linking the deformed co-ordinates to their initial positions, and the components of the transformation matrix above are directly equivalent to the values

$$\begin{pmatrix} a & b \\ c & d \end{pmatrix}$$

used in Appendix B of Ramsay & Huber (1983), where equations for the direction of principal strains of the strain ellipse (B14), finite rotation (B16), magnitude of the principal strains (B19), ellipticity (B20) and area change (B22) are conveniently listed in terms of these components.

The finite strain can also be calculated directly from three known stretches, that is from the change in length of the sides of the triangular element discussed above (e.g. Ramsay 1967, Sanderson 1977, Ramsay & Huber 1983, Ragan 1987, De Paor 1988), or from a combination of changes in angle and stretch (see Ramsay & Huber 1983 for a summary). These methods are essential for determining finite strain from deformed fossils or other strain markers, but the solution presented above is more direct when the co-ordinate positions are known, as in the analysis of deformed grids.

As shown by Hsu (1966), a two-dimensional deformation can arbitrarily be considered in terms of any combination of pure shear, simple shear and rotation. The equations relating these parameters to one another are grouped as equation (21) in that paper. In particular, the simple equation relating the value of the principal extension (as natural strain ε) to the shear strain ($\sinh \varepsilon = \gamma/2$) allows the average or bulk strain of a deformed grid to be readily expressed as either natural strain (or percentage shortening or ellipticity, if more convenient) or shear strain, whichever is more applicable to the experimental boundary conditions.

RATE OF DEFORMATION

The rate of deformation is related to variations in the velocity, that is the rate of change of position, of particles. As noted by Hsu (1967), although velocity nor-

mally means the time rate of displacement, it is more convenient in studying plastic deformation to define the rate in more general terms relative to some variable λ representing the progress of deformation. Clearly, the relationship for the velocity components $\mathbf{v}_i$ is:

$$\mathbf{v}_i = \frac{\partial \mathbf{x}_i}{\partial t} = \frac{\partial \mathbf{x}_i}{\partial \lambda}\frac{\partial \lambda}{\partial t} \tag{10}$$

and the obvious choice of variable λ would be the bulk natural strain in a constant strain rate, pure shear experiment and the bulk shear strain for a simple shear experiment. In the implementation discussed here, the user has the choice of natural strain, percentage shortening, ellipticity or shear strain as the measure of deformation. An average bulk value is calculated for each of the input digitized grids, using the overdetermined least-squares method discussed above. The rates of displacement $\partial \mathbf{x}_i/\partial \lambda$ are determined by fitting a spline curve interpolation to the values of $\mathbf{x}_i$ vs λ (cf. Ahlberg *et al.* 1967), and determining the first derivative at the particular value of λ chosen by the user for plotting (clearly plots can also be interpolated to values of bulk strain between those of the input grids). The second derivative corresponds to the acceleration $\mathbf{a}_i$ (see the section on 'spin' below). The values of velocity $\mathbf{v}_i$ can then be used to determine the velocity gradient matrix $\mathbf{v}^g_{ij} = (\partial \mathbf{v}_i/\partial \mathbf{x}_j)$, and the acceleration $\mathbf{a}_i$ the acceleration gradient matrix $\mathbf{a}^g_{ij} = (\partial \mathbf{a}_i/\partial \mathbf{x}_j)$, in the general manner established for all such vector quantities above.

As can be found in many standard texts on plasticity (e.g. Chakrabarty 1987), the principal directions of the rate of deformation make an angle θ with the x_1 axis given by

$$\tan 2\theta = \frac{v^g_{12} + v^g_{21}}{v^g_{11} - v^g_{22}} \tag{11}$$

and the magnitude of principal strain rates are given by

$$\dot{\varepsilon}_1, \dot{\varepsilon}_2 = \tfrac{1}{2}(v^g_{11} + v^g_{22}) \pm \tfrac{1}{2}\sqrt{(v^g_{11} - v^g_{22})^2 + (v^g_{12} + v^g_{21})^2}. \tag{12}$$

These values can be plotted directly (Fig. 3), or their magnitudes contoured across the surface of the model.

VORTICITY

Vorticity is defined as the curl of the velocity field (e.g. Truesdell 1954), from which it follows that the magnitude of the vorticity is given by the relation

$$|W| = v^g_{21} - v^g_{12}. \tag{13}$$

This value is equal to the combined angular velocity of those material lines which are instantaneously parallel to the principal directions of the rate of deformation. Since these lines remain instantaneously perpendicular, it is also equal to twice the angular velocity of either one of these lines taken individually (Means *et al.* 1980). Using equation (13), the magnitude of the vorticity can be determined from the off-diagonal components of the velocity gradient tensor and contoured across the surface of the model (e.g. Fig. 4).

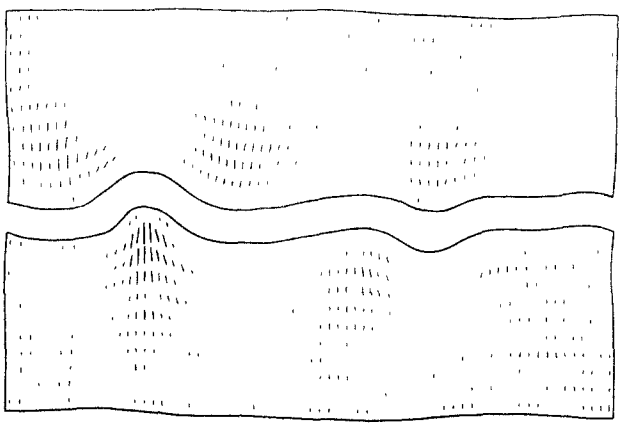

Fig. 3. Plot of the intensity of the rate of deformation within the matrix. The orientation of the line segments is parallel to the major principal axis and the length is proportional to the value of $\overline{\mathbf{II}}$, the second moment of the rate of deformation tensor (e.g Means *et al.* 1980). This is an invariant quantity related to the magnitude of the principal strain rates (equation 12), by: $\overline{\mathbf{II}} = \dot{\varepsilon}_1^2 + \dot{\varepsilon}_2^2$ This value is a measure of the intensity of the rate of deformation and appears in the denominator of the expression defining the kinematical vorticity number (equation 15)

Vorticity can only be described relative to a particular co-ordinate system, which may itself be rotating relative to some other co-ordinate system. In this sense, there is no 'absolute' value of vorticity. Reference axes can be chosen which most simplify the analysis and emphasize the physical significance. One such reference frame is that with axes parallel to the principal directions of the rate of deformation (sometimes called the stretching axes, cf. equation 11). The vorticity relative to these axes has been termed the 'internal vorticity' by Means *et al.* (1980), or the 'shear induced vorticity' by Lister & Williams (1983). The component of the vorticity related to the rotation of the stretching axes themselves relative to the chosen 'fixed' external reference frame has been termed the 'spin component' by Means *et al.* (1980) and Lister & Williams (1983), although historically the term spin has been used rather indiscriminately for any form

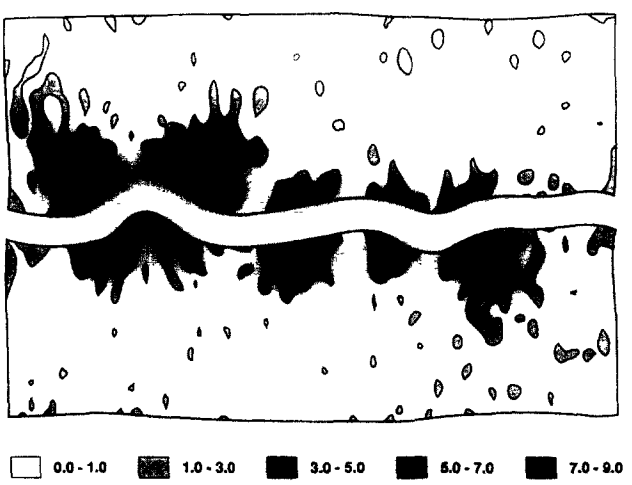

Fig 4. Contour plot of the total vorticity (equation 13) within the matrix, relative to external reference axes fixed to the frame of the deformation rig

of rotation (e.g. Truesdell 1954). To obtain a value for the 'internal vorticity', the 'spin component' must first be determined and subtracted from the total vorticity as calculated above.

The orientation of the principal directions of the rate of deformation relative to the external reference system is determined via equation (11) by the velocity gradient components. It is clear, therefore, that the orientation of these directions can only change during progressive deformation if the velocity gradient components themselves change, that is, if there are accelerations relative to the chosen reference system. The magnitude of the spin is defined as the angular velocity relative to the chosen external reference system of the two principal directions, or twice that of one such principal direction (Means *et al.* 1980). It can be derived by differentiating equation (11) with respect to λ, the measure of progressive deformation, to obtain (after some rearrangement) the angular velocity of the principal axis $\partial\theta/\partial\lambda$, and then simply multiplying by two to give the magnitude of the spin W',

$$|W'| = \frac{(a^g_{22} - a^g_{11})(v^g_{12} + v^g_{21}) + (v^g_{11} - v^g_{22})(a^g_{12} + a^g_{21})}{(v^g_{11} - v^g_{22})^2 + (v^g_{12} + v^g_{21})^2}, \tag{14}$$

where $\mathbf{a}^g_{ij}$ represent the acceleration gradient matrix components. It is clear from this equation that if all $\mathbf{a}^g_{ij}$ components are zero, the value of $|W'|$ must also be zero, and the stretching axes do not rotate in this reference frame. It is also clear that if the rate of deformation is zero, then the principal directions are indeterminate and the spin component itself is indeterminate. For very low deformation rates, the accuracy of the result for the spin value will depend markedly on the numeric precision of the variables used in the calculation (standard precision on microcomputers is usually 32 bit).

Truesdell (1953) introduced the concept of a kinematical vorticity number, which can be calculated from the vorticity and the principal stretching rates via the equation:

$$W_k = \frac{|W|}{\sqrt{2(\dot{\varepsilon}_1^2 + \dot{\varepsilon}_2^2)}}. \tag{15}$$

In the original definition, as also followed by Passchier (1987), the vorticity is the total vorticity relative to the chosen external reference frame, but Means *et al.* (1980) suggest that it would be more appropriate in studying geological structures to only include the 'internal vorticity', i.e. minus the 'spin component', in the kinematical vorticity number.

PARTITIONING OF HOMOGENEOUS AND HETEROGENEOUS FLOW COMPONENTS

The gradient tensor components $\partial \mathbf{q}_i/\partial \mathbf{x}_j$ from the general equation (1) discussed above can be fully represented by the matrix **M**. This matrix may be partitioned into a part describing the average, homogeneous distribution across the whole grid $\mathbf{M}_h$, and an additional perturbation component $\mathbf{M}_p$ superimposed upon this background value, which describes the heterogeneous variation across the grid surface. For finite values related to the displacement gradient matrix, the relationship is

$$\mathbf{M} = \mathbf{M}_p \cdot \mathbf{M}_h$$

therefore

$$\mathbf{M}_p = \mathbf{M} \cdot \mathbf{M}_h^{-1}, \tag{16}$$

where $^{-1}$ indicates the matrix inverse. The multiplication is non-commutative and the choice of order is significant. For instantaneous deformation rates related to the velocity gradient matrix the relationship is

$$\mathbf{M} = \mathbf{M}_p + \mathbf{M}_h$$

therefore

$$\mathbf{M}_p = \mathbf{M} - \mathbf{M}_h \tag{17}$$

and the choice of order is not significant. The components of $\mathbf{M}_h$ are calculated, as outlined above, by including all grid nodes in an overdetermined least-squares solution to a set of equations such as (5). The solution, using standard numerical subroutines (e.g. Lawson & Hanson 1974), is fast, even for large grids with more than 1000 nodes. The relations (16) and (17) can then be used to determine the matrix for the heterogeneous perturbation component, and these values substituted in the equations summarized above to produce plots of perturbation displacement (Fig. 5), finite strain (Fig. 6), rotation, velocity, rate of stretch, etc. These plots are particularly useful in analysing the development of mechanical instabilities such as folds, boudins and shear zones, which represent growing heterogeneities superimposed upon a basic homogeneous flow (Ramberg 1961, Biot 1965, Cobbold 1977a,b).

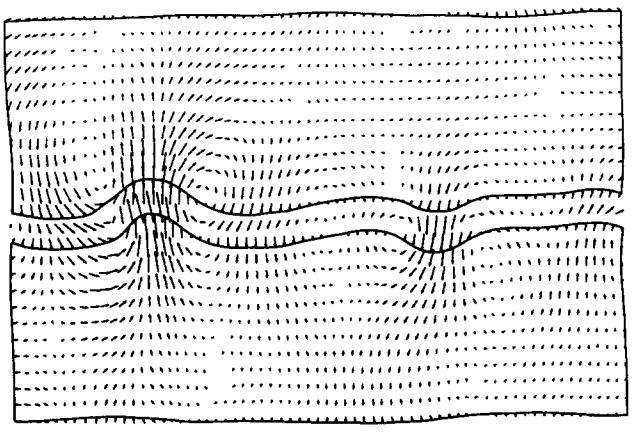

Fig. 5. Finite vector displacement field of the heterogeneous component of the deformation. The arrows join the position which would be occupied if the deformation had been homogeneous to the actual digitized position of the grid node.

CONCLUSIONS

Once the co-ordinates of known particles, conveniently represented by the nodes of an inscribed grid,

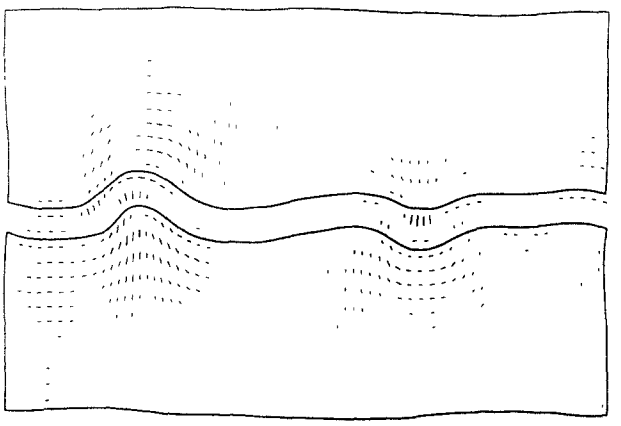

Fig 6 Plot of ln (R_p), where R_p is the ellipticity $(1 + e_1)/(1 + e_2)$ of the perturbation finite strain ellipse related to the heterogeneous component of the deformation. This logarithmic representation has a value of zero for $R_p = 1$, providing a better visual representation of the variation in the heterogeneous strain component across the surface of the model (De Paor personal communication). The plot shows very clearly the tendency for stretch parallel to the layer on the outer arc of the layer and in the adjacent matrix, with additional shortening parallel to the layer on the inner arc. This is characteristic of buckle folds both in the laboratory and in nature.

have been established at various stages of deformation by manual digitizing, much information can be extracted with little additional effort. General methods for the determination of the spatial gradients in any vector quantity can be used to calculate the displacement, velocity and acceleration gradient tensor components. Finite values of strain, rotation and area change can then be calculated from the displacement gradients, values of the instantaneous rate of deformation, vorticity and rate of area change from the velocity gradients, and values of the spin of the stretching axes from a combination of velocity gradients and acceleration gradients. These values may then be factorized into a background homogeneous component and a superimposed heterogeneous component, which allows a more direct investigation of the progressive development of mechanical instabilities such as folds, boudins and shear zones.

Acknowledgements—The analogue model experiment used as an example was performed by Mohammad Abbassi as part of a more extensive investigation of single-layer folding. Criticism of earlier drafts by Declan De Paor, Dave Sanderson, Lisa Dell'Angelo, Martin Casey, Benoit Ildefonse and John Ramsay is gratefully acknowledged Financial support was provided by Swiss National Fonds Project 21-25258 88

REFERENCES

Ahlberg, J , Nilson, E & Walsh, J. 1967. *The Theory of Splines and Their Applications*. Academic Press, New York.

Biot, M A 1965. *Mechanics of Incremental Deformations*. John Wiley & Sons, New York

Chakrabarty, J 1987 *Theory of Plasticity*. McGraw-Hill, New York

Cobbold, P R 1975 Fold propagation in single embedded layers *Tectonophysics* **27**, 333–351

Cobbold, P R 1977a Description and origin of banded deformation structures I Regional strain, local perturbations, and deformation bands *Can J Earth Sci* **14**, 1721–1731

Cobbold, P R 1977b Description and origin of banded deformation structures II Rheology and the growth of banded perturbations *Can. J Earth Sci* **14**, 2510–2523

De Paor, D G 1988 Strain determination from three known stretches—an exact solution *J Struct Geol* **10**, 639–642

Dixon, J M 1974 A new method of determining finite strain in models of geological structures *Tectonophysics* **24**, 99–114

Fitz Gerald, J. D & Chopra, P N. 1984 Distribution of strain in some geological materials experimentally deformed at high pressure and temperature In· *Deformation of Ceramic Materials II* (edited by Tressler, R E & Bradt, R. C) Plenum Press, New York, 321–328.

Gairola, V K 1978. Strain distribution across an experimental single-layer fold. *Tectonophysics* **44**, 27–40.

Ghosh, S K 1975 Distortion of planar structures around rigid spherical particles *Tectonophysics* **28**, 185–208

Ghosh, S. K & Ramberg, H. 1976 Reorientation of inclusions by combination of pure shear and simple shear *Tectonophysics* **34**, 1–70

Hudleston, P J 1973 An analysis of 'single layer' folds developed experimentally in viscous media. *Tectonophysics* **16**, 189–214.

Hsu, T C 1966 A study of large deformations by matrix algebra. *J Strain Analysis* **1**, 313–321

Hsu, T. C 1967 Velocity field and strain-rates in plastic deformation. *J Strain Analysis* **2**, 196–206.

Jaeger, J. C 1962 *Elasticity, Fracture and Flow* (2nd edn). Methuen, London

Lawson, C L & Hanson, R J 1974 *Solving Least Squares Problems* Prentice-Hall, Englewood Cliffs, New Jersey

Lister, G. S. & Williams, P F 1983 The partitioning of deformation in flowing rock masses *Tectonophysics* **92**, 1–33

Malvern, L E. 1969. *Introduction to the Mechanics of a Continuous Medium*. Prentice-Hall, Englewood Cliffs, New Jersey

Mancktelow, N S. 1988. An automated machine for pure shear deformation of analogue materials in plane strain *J Struct Geol* **10**, 101–108

Means, W D. 1983 Microstructure and micromotion in recrystallization flow of octachloropropane, a first look *Geol Rdsch* **72**, 511–528

Means, W D , Hobbs, B E , Lister, G S & Williams, P F. 1980. Vorticity and non-coaxiality in progressive deformations *J Struct. Geol* **2**, 371–378

Neurath, C & Smith, R B 1982 The effect of material properties on growth rates of folding and boudinage· experiments with wax models. *J Struct. Geol* **4**, 215–229

Passchier, C. W 1987 Stable positions of rigid objects in non-coaxial flow—a study in vorticity analysis. *J Struct Geol* **9**, 679–690.

Ragan, D. M 1987 Strain from three measured stretches *J. Struct. Geol.* **9**, 897–898

Ramberg, H 1959 Evolution of ptygmatic folding *Norsk geol Tidsskr* **39**, 99–151

Ramberg, H 1961 Contact strain and folding instability of a multilayered body under compression *Geol Rdsch.* **51**, 405–439.

Ramberg, H 1963 Fluid dynamics of viscous buckling applicable to folding of layered rocks *Bull Am Ass Petrol. Geol* **47**, 484–515.

Ramberg, H. 1964 Strain distribution and geometry of folds. *Bull. geol Inst Univ. Uppsala* **42**, 1–20

Ramsay, J G 1967 *Folding and Fracturing of Rocks* McGraw-Hill, New York

Ramsay, J G & Huber, M I 1983 *The Techniques of Modern Structural Geology, Volume* 1 *Strain Analysis* Academic Press, London

Sanderson, D J 1977 The algebraic evaluation of two-dimensional finite strain rosettes. *Math Geol* **9**, 483–496

Truesdell, C 1953. Two measures of vorticity. *J Rational Mech & Analysis* **2**, 173–217

Truesdell, C. 1954 *The Kinematics of Vorticity* Indiana University Press, Bloomington, Indiana